SLAC – PUB – 3549
January 1985
(T/E)

SEARCH FOR HIGGS BOSON IN TOPONIUM DECAYS*

M. CHAICHIAN

Department of High Energy Physics,
University of Helsinki, Helsinki, Finland

and

M. HAYASHI†

Stanford Linear Accelerator Center
Stanford University, Stanford, California, 94305

ABSTRACT

We study the decays of toponium V, with particular attention to Higgs–boson production. Decay modes such as $V \to \gamma^*$, $Z^0 \to H\gamma$, $V \to \gamma^*$, $Z^0 \to H^3S_1(\Upsilon, \Psi)$ and $V \to Z^0 \to H\ell^+\ell^-$ are also considered. These rates are found to be very small in the minimal (one-Higgs – doublet) model. We discuss shortly the consequences of a composite model for the Higgs boson and of enhanced coupling constants of a light Higgs boson to fermions in a two-Higgs – doublet scheme. The implications of a possible mixing between V and Z^0 on the production of V in e^+e^- – collisions as well as in $\bar{p}p$ – collisions are considered.

Submitted to *Physical Review D*

---

*Work supported by the Department of Energy, contract DE-AC03-76SF00515.

† Permanent address: Department of Physics, Saitama Medical College, Saitama 350-04, JAPAN.

1. INTRODUCTION

One of the most important questions in particle physics today, after the discovery of the W and Z bosons at the CERN $\bar{p}p$ collider and possibly the top quark,[1-3] is whether the Higgs boson, an important feature of the standard model, does exist or not. It has been known since Wilczek's work[4] in 1977 that a heavy quarkonium can provide a possible laboratory for studying neutral light Higgs – boson production. The search for a Higgs boson in the decay products of quarkonia has attracted much renewed interest recently in connection with the so-called $\varsigma(8.3)$[5] whose existence, though, is now doubtful. In this paper, we will study the decays of toponium $V(t\bar{t})$, paying particular attention to the light Higgs–boson production. Such study exists in the literature.[6] Many earlier calculations, however, have been restricted to the lower mass region of the top–quark m_t. We will study the toponium decays in the range $30 \leq m_t \leq 60$ GeV, (according to $UA1$,[3] $30 \leq m_t \leq 50$ GeV), taking into account the Z^0–boson effect in the main decay modes of the V : $V \to \gamma^*$, $Z^0 \to \sum_f f\bar{f}$, $\sum_\ell \ell^+\ell^-$ (f = quark and ℓ = lepton) and a possible $V - Z^0$ mixing. The Z^0–boson contribution gives strong effects on the branching ratios of decay modes in the vicinity of $m_t \sim M_Z/2$.

We organize the paper as follows: In Sec. 2 we review shortly the known formulas for various decay modes of V taking into account the contribution of Z^0. We will devote special attention to decay modes of the V : $V \to \gamma^*$, $Z^0 \to H\gamma$, $V \to \gamma^*$, $Z^0 \to H\ {}^3S_1(\Upsilon, \Psi)$ and $V \to Z^0 \to H\ell^+\ell^-$ for which we derive the formulas in Sec. 3. The formula for the decay width of the particular process $V \to \gamma^*$, $Z^0 \to H\gamma$ is also derived in a composite model for the Higgs scalar. Section 4 is devoted to the numerical results for the processes presented in Secs. 2

and 3. The decay rates for these processes are found to be extremely small in the minimal Higgs model. We will discuss shortly the consequences of a composite model for the Higgs boson and of enhanced coupling constants to fermions which arise if the H appears to be a light scalar one in a two-Higgs–doublet scheme. In Sec. 5 we discuss the implications of the possible $V - Z^0$ mixing on the production of V in e^+e^-–collisions as well as in $\bar{p}p$–collisions. Section 6 is devoted to conclusions.

2. REVIEW OF BASIC FORMULAS

In the following we present the formulas for each decay mode of the toponium, together with the corresponding diagrams illustrating the decay mechanisms. Restricted formulas for the cases (1) - (9) below can be found in Ref. 6.

(1) $V \to \gamma^*,\ Z^0 \to f\bar{f}$ (f = quark) (Fig. 1).

$$\Gamma(V \to \gamma^*,\ Z^0 \to f\bar{f}) = \frac{9}{2} v_f \left(1 + \frac{\alpha_S(M_V)}{\pi}\right) e_f^2 \left[\left(1 - \frac{v_f^2}{3}\right) K_f - \frac{(1 - v_f^2) A_t^2 B_f^2 |D_Z|^2 M_V^4}{e_t^2 e_f^2 \sin^4\theta_W \cos^4\theta_W}\right] \Gamma_{o\ell}\ , \tag{1}$$

where

$$\Gamma_{o\ell} = \Gamma(V \to \gamma^* \to \ell^+\ell^-)\ ,$$

$$K_f = \left|1 - \frac{A_t A_f M_V^2 D_Z}{e_t e_f \sin^2\theta_W \cos^2\theta_W}\right|^2 + \left|\frac{A_t B_f M_V^2 D_Z}{e_t e_f \sin^2\theta_W \cos^2\theta_W}\right|^2\ ,$$

$$D_Z = \frac{1}{(M_V^2 - M_Z^2) + iM_Z\Gamma_Z}\ ,$$

$$v_f = \sqrt{1 - 4m_f^2/M_V^2}\ ,$$

for

$$f = u, c, t; \quad e_f = \tfrac{2}{3}, \quad A_f = \tfrac{1}{4} - \tfrac{2}{3}\sin^2\theta_W, \quad B_f = \tfrac{1}{4},$$
$$f = d, s, b; \quad e_f = -\tfrac{1}{3}, \quad A_f = -\tfrac{1}{4} + \tfrac{1}{3}\sin^2\theta_W, \quad B_f = -\tfrac{1}{4}.$$

(2) $V \to \gamma^*,\ Z^0 \to \ell^+\ell^-$ ($\ell = e,\ \mu,\ \tau$) (Fig. 2).

$$\Gamma(V \to \gamma^*,\ Z^0 \to \ell^+\ell^-) = \Gamma_{0\ell} \cdot f_R(\alpha_S) K_\ell \ , \tag{2}$$

where

$$f_R(\alpha_S) = 1 - \frac{16\alpha_S}{3\pi} \ ,$$

$$K_\ell = \left|1 - \frac{A_t a_\ell M_V^2 D_Z}{e_t \sin^2\theta_W \cos^2\theta_W}\right|^2 + \left|\frac{A_t b_\ell M_V^2 D_Z}{e_t \sin^2\theta_W \cos^2\theta_W}\right|^2 \ ,$$

$$a_\ell = -\frac{1}{4} + \sin^2\theta_W \ , \ b_\ell = -\frac{1}{4} \ .$$

(3) $V \to Z^0 \to \nu_\ell \bar{\nu}_\ell$ (Fig. 3).

$$\Gamma(V \to Z^0 \to \nu_\ell \bar{\nu}_\ell) = \frac{\Gamma_{0\ell} A_t^2 (a_\nu^2 + b_\nu^2) |D_Z|^2 M_V^4}{e_t^2 \sin^4\theta_W \cos^4\theta_W} \ , \tag{3}$$

where

$$a_\nu = \frac{1}{4}, \ b_\nu = \frac{1}{4} \ .$$

(4) $V \to 3g$ (Fig. 4).

$$\Gamma(V \to 3g) = \frac{10}{81} \frac{\pi^2 - 9}{\pi} \cdot \frac{\alpha_S^3}{\alpha^2} \cdot \frac{\Gamma_{0\ell}}{e_t^2} \ . \tag{4}$$

(5) $V \to 2g\gamma$ (Fig. 5).

$$\Gamma(V \to 2g\gamma) = \frac{36}{5} e_t^2 \frac{\alpha}{\alpha_S} \Gamma(V \to 3g) \ . \tag{5}$$

(6) $V \to t\bar{t} \to tW^-\bar{b}$ (Fig. 6).

$$\Gamma_{W1} = \frac{9(\sqrt{2}G_F)^2}{192\pi^3}\, m_t^5 \left(1+\frac{m_t^2}{M_W^2}\right)^{-2} . \tag{6}$$

(7) $V \to b\bar{b}$ (weak decay) (Fig. 7).

$$\Gamma_{W2} = \frac{3\eta_W^2 |U_{tb}|^4\, M_V^4\, \Gamma_{0\ell}}{32\, e_t^2\, \sin^4\theta_W\, \cos^4\theta_W\, M_Z^4} , \tag{7a}$$

where

$$\eta_w = \frac{1}{3}\left(1+\frac{1}{8}\frac{M_V^2}{M_W^2}\right) \Big/ \left(1+\frac{M_V^2}{4M_W^2}\right) ,$$

U_{tb} = the Kobayashi – Maskawa quark mixing matrix element for the $t \to b$ transition.

The interference terms between $V \to \gamma^*$, $Z^0 \to b\bar{b}$ and $V \to b\bar{b}$ (weak decay) are given by

$$\Gamma_{W3} = \Gamma_{\gamma^*-W}(V \to b\bar{b}) + \Gamma_{Z-W}\ (V \to b\bar{b}) , \tag{7b}$$

where

$$\Gamma_{\gamma^*-W}(V \to b\bar{b}) = -\frac{3e_b M_V^2 |U_{tb}|^2\, \eta_w \Gamma_{0\ell}}{4e_t\, \sin^2\theta_W\, \cos^2\theta_W\, M_Z^2} ,$$

$$\Gamma_{Z-W}(V \to b\bar{b}) = -\frac{3A_t(A_b+B_b)\, M_V^4 ReD_Z \cdot |U_{tb}|^2\, \eta_w}{4e_t^2\, \sin^4\theta_W\, \cos^4\theta_W\, M_Z^2} .$$

(8) $V \to H\gamma$ (Wilczek's mechanism) (Fig. 8).

$$\Gamma_{Wilczek}(V \to H\gamma) = \frac{\sqrt{2}G_F M_V^2}{8\pi\alpha}\left(1-\frac{m_H^2}{M_V^2}\right)\Gamma_{0\ell} . \tag{8}$$

3. THE DECAYS OF V INTO A HIGGS BOSON

Now we consider several decays of V into a scalar H.

(9) $V \to \gamma^*,\ Z^0 \to H\gamma$ (loop diagrams, Fig. 9).

In addition to the Wilczek's mechanism, the fermion and W-boson loop diagrams of Fig. 9 can contribute to the decay channel $V \to H\gamma$ (the crossed diagrams are not shown). The decay width can be expressed as:

$$\Gamma_{loop}(V \to \gamma^*,\ Z^0 \to H\gamma) = \Gamma_{0\ell} \cdot \frac{\sqrt{2}\, G_F \alpha M_V^2}{8\pi^3} \left(1 - \frac{m_H^2}{M_V^2}\right)^3 |J|^2 \ , \qquad (9a)$$

where

$$J = \sum_f I_f \left(1 - \frac{A_t A_f M_V^2 D_Z}{e_t e_f \sin^2\theta_W \cos^2\theta_W}\right) - I_W \left(1 + \frac{A_t \cot\theta_W M_V^2 D_Z}{e_t \sin\theta_W \cos\theta_W}\right) \ ,$$

$$I_f = m_f^2 \cdot 3^{c_f} \cdot e_f^2 \int_0^1 dx \int_0^{1-x} \frac{1 - 4xy}{m_f^2 - M_V^2 y(1-x-y) - m_H^2 xy - i\epsilon} \ ,$$

$$I_W = M_W^2 \int_0^1 dx \int_0^{1-x} \frac{2[\lambda - \rho xy]}{M_W^2 - M_V^2 y(1-x-y) - m_H^2 xy - i\epsilon} \ ,$$

$$\lambda = 2 - M_V^2/2M_W^2 \ ,$$

$$\rho = 3 - \frac{(M_V^2 - m_H^2)}{2M_W^2} - \frac{M_V^2 m_H^2}{4M_W^4} \ ,$$

$$c_f \text{ (color factor)} = \begin{cases} 1 & \text{for quarks} \\ 0 & \text{for leptons} \end{cases}$$

The integration in I_f and I_W can be carried out analytically.[7]

The contribution from the interference between the Wilczek type mechanism and the loop diagrams reads as:

$$\Gamma_{int}(\text{Wilczek type} \otimes \text{loops}) = -\Gamma_{0\ell}\frac{M_V^2\sqrt{2}G_F}{4\pi^2}\left(1-\frac{m_H^2}{M_V^2}\right)^2 ReJ\ . \qquad (9b)$$

(10) $V \to \gamma^*,\ Z^0 \to H^3S-1\ (^3S_1 = \Upsilon, \Psi)$ (Fig. 10).

Neglecting for simplicity the γ^* contribution in the loop diagram of Fig. 10a, the decay width can be given as:

$$\Gamma(V \to Z^0 \to\ H\ ^3S_1) = \Gamma_{0\ell}\cdot\frac{A_t^2|D_Z|^2M_V^4}{e_t^2\sin^4\theta_W\cos^4\theta_W}\ R_H(^3S_1). \qquad (10a)$$

We take $R_H(^3S_1)$ from Ref. 8, which has been calculated adopting a non-relativistic bound-state picture for describing the quarkonia. In out notation it reads as:

$$R_H(^3S_1) = \frac{C_H A_f^2\omega}{(1+\mu_H^2-\mu^2)^2}\left\{\left[1-\mu^2+\mu_H^2\,\frac{2\mu^2-\mu_H^2}{1-\mu^2}\right]^2 + 2\mu^2\left[1-\mu^2+\mu_H^2\,\frac{3-\mu^2}{1-\mu^2}\right]^2\right\}, \qquad (10b)$$

where

$$f = b(c),\ \text{ for }\ ^3S_1 = \Upsilon(\Psi),$$

$$\mu_H^2 = m_H^2/M_V^2,\ \ \mu^2 = M^2/M_V^2\ \ (M:\ \text{the mass of}\ ^3S_1),$$

$$\omega = \left\{\ (1-\mu^2)^2 - \mu_H^2(2+2\mu^2-\mu_H^2)\right\}^{1/2}\ .$$

Using the empirical regularity:[8]

$$\Gamma(^3S_1 \to e^+e^-)/e_f^2 \simeq 10^{-5}\ \text{GeV},$$

which is known to be satisfied quite well, we have

$$C_H = 1.8 \times 10^{-7} M.$$

The decay widths of the V into other quarkonium states such as $^1S_0$, $^3P_1$, etc. can also be calculated similarly.

(11) $V \to Z^0 \to H\ell^+\ell^-$ (Fig. 11).

A straightforward calculation leads us to the following decay width:

$$\Gamma(V \to Z^0 \to H\ell^+\ell^-) = \frac{\alpha M_V^2 M_Z^2 A_i^2 (a_\ell^2 + b_\ell^2)}{48\pi \sin^6\theta_W \cos^6\theta_W} \cdot \Gamma_{0\ell} |D_Z|^2$$

$$\cdot \int_0^{(1-m_H/M_V)^2} dx \frac{[x^2 - 2(1+\mu_H^2)x + (1-\mu_H^2)^2]^{1/2}}{(x-\mu_Z^2)^2 + \Gamma_Z^2 \mu_Z^2 / M_V^2} \qquad (11)$$

$$\cdot [x^2 + (10 - \mu_H^2)x + (1-\mu_H^2)^2],$$

where

$$\mu_Z^2 = M_Z^2 / M_V^2 \ .$$

One can derive the decay widths for the processes $V \to Z^0 \to H\nu\bar{\nu}$ and $V \to Z^0 \to Hf\bar{f}$ (f = quarks) in a similar way.

(12) $V \to \gamma^*$, $Z^0 \to H\gamma$ (composite Higgs, Fig. 12).

Finally, we consider the process $V \to \gamma^*$, $Z^0 \to H\gamma$ in a model for composite Higgs.[9] In composite models where vector bosons ($W^\pm$, Z^0) and scalar boson H are made of the same subconstituents, the couplings like $HZ\gamma$, $H\gamma\gamma$ and Hgg could be completely different from the standard (minimal) Higgs case.[9] (The other couplings like $Hf\bar{f}$, HWW and HZZ are similar to the standard Higgs

couplings). If one assumes additionally the W-dominance model[10] for photon–hadron interaction, the couplings of H to two vector states $f_{HVV'}$ reads as:

$$f_{H\gamma\gamma} = \sin^2\theta_W / M_W \ ,$$
$$f_{HZ\gamma} = \sin\theta_W / M_W \ , \tag{12a}$$

where we use the gauge invariant form

$$f_{HVV'}\left((e\cdot e')(k\cdot k') - (ek')(e'k)\right)$$

with e^μ, e'^μ, k^μ and k'^μ being polarizations and momenta of the vector states, respectively. Then the decay width is given by:

$$\Gamma_{\text{composite}}(V\to\gamma^*,\ Z^0\to H\gamma) = \Gamma_{0\ell}\cdot\frac{M_V^2}{32\pi\alpha}\left(1-\frac{m_H^2}{M_V^2}\right)^3 \cdot\left|f_{H\gamma\gamma} - \frac{M_V^2 f_{HZ\gamma} D_Z A_t}{\sin\theta_W\ \cos\theta_W}\right|^2 \ . \tag{12b}$$

The contribution from the interference between the diagrams of Fig. 8 and Fig. 12 reads as:

$$\Gamma_{\text{int.}}(\text{Wilczek type}\ \otimes\ \text{composite}) = -\Gamma_{0\ell}\cdot\frac{M_V^2(\sqrt{2}G_F)^{1/2}}{8\pi\alpha}\left(1-\frac{m_H^2}{M_V^2}\right)^2 \cdot Re\left\{\ f_{H\gamma\gamma} - \frac{f_{HZ\gamma}A_t\ M_V^2 D_Z}{\sin\theta_W\ \cos\theta_W}\right\} \ . \tag{12c}$$

Although we restrict ourselves to a discussion for $V\to\gamma^*$, $Z^0\to H\gamma$ in this paper we note that in composite models for Higgs–boson, the processes like $V\to\overline{\gamma^*}$, $Z^0\to H^3S_1$ and $V\to\gamma^*$, $Z^0\to H\ell^+\ell^-$ (Fig. 13) etc. can give nonnegligible contributions.

4. NUMERICAL RESULTS

Numerical calculations for the decay widths and the branching ratios are performed by employing the following values:

$$\alpha_S(M_V) = \frac{0.193}{1 + \frac{21}{12\pi} \cdot 0.193 \ell n \left(\frac{M_V}{3.1}\right)^2}, \quad \sin^2\theta_W = 0.226,$$

$m_H = 8.3$ GeV (we assume this value as a representative one), $M_Z = 92.4$ GeV, $\Gamma_Z = 2.87$ GeV, $m_u = 4 \cdot 10^{-3}$ GeV, $m_d = 7.5 \cdot 10^{-3}$ GeV, $m_s = 0.15$ GeV, $m_c = 1.5$ GeV, $m_b = 4.5$ GeV, $\Gamma_{0\ell} = \Gamma(V \to \gamma^* \to \ell^+\ell^-) = 5$ keV, $M_W = 81$ GeV, $U_{tb} = 1$, $\Gamma(\Upsilon \to \gamma^* \to \ell^+\ell^-) = 1.6$ keV, $M_\Upsilon = 9.46$ GeV, and $M_\Psi = 3.1$ GeV. We show the curves for the decay widths and the corresponding branching ratios as a function of m_t in Figs. 14 - 18. In Figs. 16 and 17 we compare the decay width $\Gamma(V \to H\gamma)$ by different mechanisms and the interference contributions $\Gamma_{int}(V \to H\gamma)$. In Fig. 19 we plot the branching ratios for the decays of V into H as a function of m_H.

A few remarks are in order.

i) The rates for the decay processes (9) and (10) are unfortunately extremely small in the minimal one-Higgs – doublet model:

$$\frac{\Gamma_{loop}(V \to \gamma^*,\ Z^0 \to H\gamma)}{\Gamma_{Wilczek}(V \to H\gamma)} \lesssim 10^{-2},$$

$$\frac{\Gamma(V \to \gamma^*,\ Z^0 \to H\Upsilon)}{\Gamma_{Wilczek}(V \to H\gamma)} \lesssim 10^{-4}, \qquad (13)$$

$$\frac{\Gamma(V \to \gamma^*,\ Z^0 \to H\Psi)}{\Gamma_{Wilczek}(V \to H\gamma)} \lesssim 10^{-5}.$$

ii) The branching ratio $B(V \to H\gamma)$ due to Wilczek's mechanism is strongly dependent on m_t and takes a minimum value of $\sim 5 \cdot 10^{-4}$ when $m_t \to M_Z/2$,

which is comparable with $B(\Upsilon \to H\gamma) \sim 8 \cdot 10^{-4}$. Outside the vicinity of $m_t \sim M_t/2$, it takes the value $B(V \to H\gamma) \sim 10^{-2}$.

iii) In a two– or multi-Higgs – doublet scheme a light Higgs scalar can have enhanced coupling constant to fermions. Such a possibility has attracted a renewed interest[11] recently in an attempt to interpret the $\xi(2.2)$ and the so-called $\varsigma(8.3)$.[5] Here we have considered a two- or multi-Higgs doublet model in which the couplings of H to fermions are all enhanced by a factor of $1/\beta \sim 12$ compared with the ones in the minimal model while the couplings of H to bosons ($W^{\pm}$, Z^0) are suppressed by the same factor. The branching ratios are plotted in Fig. 20, assuming the enhancement factor[11] $1/\beta = 12$. Outside the vicinity of $m_t \sim M_Z/2$, the decay $V \to H\gamma$ via the Wilczek mechanism becomes even a dominating one. In Fig. 16 some of the widths are shown also with this enhancement factor.

iv) In a composite model for Higgs considered above the dependence of branching ratios are depicted in Fig. 21 as a function of m_t. As seen from Figs 21 and 18, the branching ratios of many channels are quite similar in the composite and in the minimal model. In Fig. 16 the width of one channel is given in the composite scheme. For completeness the contribution of the interference term to the width of $V \to H\gamma$ channel is shown as a function of m_t in Fig. 22.

5. EFFECTS OF $V - Z^0$ MIXING ON PRODUCTION OF V

Now let us consider the production of the V. For m_t very close to $M_Z/2$, mixing would cause the enhanced production of V:

in e^+e^- - collisions

We have at the peak of the resonance:

$$r_{e^+e^-} = \frac{\int_{\rm res} \sigma(e^+e^- \to V)ds}{\int_{\rm res} \sigma(e^+e^- \to Z^0)ds} = \frac{M_Z}{M_V} \frac{\Gamma(V \to e^+e^-)}{\Gamma(Z^0 \to e^+e^-)}. \qquad (14)$$

With the "bare" width $\Gamma(V \to \gamma^* \to e^+e^-) = 5$ keV and the standard value $\Gamma(Z^0 \to e^+e^-) = 86.4$ MeV, we find $r_{e^+e^-} = 0.6 \cdot 10^{-4}$. With the realistic mixing $|\phi| \sim 0.2$ one has $r_{e^+e^-} = \tan^2|\phi| \simeq 0.04$, hence giving an enhancement factor ~ 700. If such a mixing of V and Z^0 occurs, then the minimum observed in $B(V \to H\gamma)$ in the vicinity of $m_t \sim M_Z/2$ (*cf* Figs. 18, 20 and 21) would be compensated, thus making the production rate for $e^+e^- \to V \to H\gamma$ a sizeable value.

in $\bar{p}p$ - collisions

We have[13]

$$r_{\bar{p}p} = \frac{\sigma(\bar{p}p \to V)}{\sigma(\bar{p}p \to Z^0)} = \begin{cases} 0.004 & \text{(no enhancement due to mixing)} \\ 0.04 & \text{(a realistic mixing with } |\phi| = 0.2) \\ 1.0 & \text{(maximal mixing).} \end{cases} \qquad (15)$$

Thus, we gain the enhancement factor of $\sim 10 - 250$. On the other hand, we have a rapidly changing value of $B(V \to H\gamma)$ in the vicinity of $m_t \sim M_Z/2$ dependent on m_t, i.e. $B(V \to H\gamma) \sim 6 \cdot 10^{-4} - 2 \cdot 10^{-2}$ (*cf* Fig. 18). Thus we expect the

production rate for the Higgs boson to be roughly

$$\sigma(\bar{p}p \to V \to H\gamma)/\,\sigma(\bar{p}p \to Z^0 \to \mu^+\mu^-) \sim (2 \cdot 10^{-2} - 1)\; r_{\bar{p}p}, \qquad (16)$$

with $B(Z^0 \to \mu^+\mu^-) = 3\%$. Consequently the search for the Higgs–boson in the (minimal) single-Higgs – doublet model using the reaction $\bar{p}p \to V \to H\gamma$ would be feasible only with considerably high luminosity beams.

The branching ratios of the Higgs boson decays in the minimal Higgs-boson model with $m_H = 8.3$ GeV are:

$$\begin{aligned} B(H \to \tau^+\tau^-) &= 0.26, \\ B(H \to \bar{c}c) &= 0.60, \\ B(H \to \mu^+\mu^-) &= 1.10^{-3}, \\ B(H \to gg) &= 0.14. \end{aligned} \qquad (17)$$

The total decay width is $\Gamma_{tot}(H) = 47$ keV. In the two- or multi-Higgs – doublet model considered above we have the same branching ratios as in Eq. (17), but the total decay width is now $\Gamma_{tot}(H) \sim 6$ MeV. In this case we find

$$\frac{\sigma(\bar{p}p \to V \to H\gamma)}{\sigma(\bar{p}p \to Z^0 \to \mu^+\mu^-)} \sim (2 - 26) r_{\bar{p}p}. \qquad (18)$$

In a composite model for the Higgs boson[9] these values could change considerably if the branching ratios for $H \to \gamma\gamma$ and/or $H \to gg$ become much larger than the ones of the minimal Higgs model, which gives $\Gamma(H \to \gamma\gamma) \sim 2$ eV and $\Gamma(H \to gg) \sim 6.5$ keV. Within a nonrelativistic formulation for a composite

scalar H in terms of bound state wave functions at the origin[9] one has:

$$B(H \to \tau^+\tau^-) = 9 \cdot 10^{-4},$$

$$B(H \to \bar{c}c) = 2 \cdot 10^{-3},$$

$$B(H \to \gamma\gamma) = 99.7, \tag{19}$$

$$\Gamma_{\rm tot}(H) \sim 14 \text{ MeV}.$$

If the subconstitutents are colored, then one has

$$B(H \to \gamma\gamma) = 3 \cdot 10^{-3},$$

$$B(H \to gg) = 99.7, \tag{20}$$

$$\Gamma_{\rm tot}(H) \sim 5 \text{ GeV}.$$

In this case the Higgs boson can be produced copiously in $\bar{p}p$ collision through gluon – gluon fusion. The production rate for the Higgs boson via $V \to H\gamma$ is

$$\sigma(\bar{p}p \to V \to H\gamma)/\sigma(\bar{p}p \to Z \to \mu^+\mu^-) \lesssim 0.9\, r_{\bar{p}p}\ . \tag{21}$$

Now let us make a remark concerning the detection of H through $H \to f\bar{f}(f = c, \tau)$. In the case of $\bar{c}c\gamma$ channel, the invariant mass of the $\bar{c}c$ pair can be, in principle, measured (although approximately), since the products of $\bar{c}c$ decays should look like a single jet with a hard photon associated with it.[14] In the case of the $\tau^+\tau^-\gamma$ channel, however, although the $\tau^+\tau^-$ decay products would again look like a single jet, a part of the energy – momentum, due to neutrinos, would be missing. Thus the observed jet energy – momentum would have a misbalance against the associated hard photon. This makes the invariant mass measurement of $\tau^+\tau^-$ decay products more uncertain.

The situation would become immensely more favorable, of course, when vertex detector is put into operation. In that case the $\bar{c}c$ and $\tau^+\tau^-$ tracks can be individually identified. Thus one would have a characteristic signature of a hard photon recoiling against two identified $\bar{c}c$ or $\tau^+\tau^-$ tracks with a narrow opening angle, which would in turn determine the invariant mass.

6. CONCLUSIONS

We have studied in detail the different mechanisms for the decay of toponium state into various channels in particular the channels including a light Higgs boson. As preliminary data indicate the mass of toponium might be not too far from the Z^0 mass. Therefore, there might exist a considerable mixing between the two states. In this respect, we have considered the enhanced production rates of toponium state in hadron–hadron collisions and its subsequent decay into a Higgs boson. Such a mechanism for the production of Higgs boson is quite favorable since one has a double enhancement operating: the first one is the enhanced production of Z^0 and its mixing with Z^0; the second enhancement is the usual large coupling of the Higgs boson to quarks. Several interesting channels have been pointed out which could make the experimental detection of light Higgs boson feasible. The same mechanism is operative in the case of e^+e^- collisions at the mass near to the toponium as discussed in Sec. 5.

ACKNOWLEDGEMENTS

We are indebted to K. Katsuura, R. Kinnunen, J. Lindfors, K. Nishikawa, F. Ochiai, R. Orava, D. P. Roy and B. Ward for enlightening discussions and correspondence. We thank SLAC theory group for the hospitality.

REFERENCES

1. G. Arnison et al., Phys. Lett. 122B (1983) 103; M. Banner et al., Phys. Lett. 122B (1983) 476.
2. G. Arnison et al., Phys. Lett. 126B (1983) 398; P. Bagnaia et al., Phys. Lett. 129B (1983) 130.
3. C. Rubbia, Talk given at the 11th International Conference on Neutrino Physics and Astrophysics, Dortmund (1984).
4. F. Wilczek, Phys. Rev. Lett. 39 (1977) 1304.
5. Crystall Ball Collaboration, DESY-84-064 and SLAC-PUB-3380 (1984).
6. K. Fujikawa, Prog. Theor. Phys. 61 (1979) 1186; J. Ellis, M. K. Gaillard, D. V. Nanopoulos and C. T. Sachrajda, Phys. Lett. 83B (1979) 339; S. Pakvasa, M. Dechantsreiter, F. Halzen and D. M. Scott, Phys. Rev. D20 (1979) 2862; Phys. Rev. D21 (1980) 1439 (E); G. Goggi and G. Penso, Nucl. Phys. B165 (1980) 429; I. I. Y. Bigi and H. Krasemann, Z. Phys. C7 (1981) 127; L. M. Sehgal and P. M. Zerwas, Nucl. Phys. B183, (1981) 417; W. Buchmüller and S. -H. H. Tye, Phys. Rev. D24 (1981) 132; J. P. Leveille, in "Proceedings of the Cornell Z^0 Theory Workshop," ed. by M. E. Peskin and S. -H. H. Tye (1981). J. D. Jackson, S. Olsen and S. -H. H. Tye, in "Proceedings of 1982 DPF Summer Study on Elementary Particle Physics and Future Facilities," ed. by R. Donaldson, R. Gustafson and F. Paige, (1982).
7. J. P. Leveille, Phys. Lett. 83B (1979) 123.
8. B. Guberina, J. H. Kühn, R. D. Peccei and R. Rückl, Nucl. Phys. B174 (1980) 317.

9. F. M. Renard, Phys. Lett. 126B (1983) 59.

10. R. Kögerler and D. Schildknecht, CERN-TH-3231 (1982); M. Kuroda and D. Schildknecht, Phys. Lett. 121 (1983) 173.

11. S. L. Glashow and M. Machacek, Phys. Lett. 145B (1984) 302; H. E. Haber and G. L. Kane, Phys. Lett. 135B (1984) 196; R. M. Barnett, G. Senjanović, L. Wolfenstein and D. Wyler, Phys. Lett. 136B (1984) 191; R. M. Barnett, G. Senjanović and D. Wyler, Phys. Rev. D20 (1984) 1529; R. S. Willey, Phys. Rev. Lett. 52 (1984) 585; K. D. Lane, S. Meshkov and F. Wilczek, Phys. Rev. Lett. 53 (1984) 1718; H. Georgi, A. Manohar and G. Moore, Phys. Lett. 149B (1984) 234; H. E. Haber and G. L. Kane, UMTH-84-26; M. Shin, H. Georgi and M. Axenides, HUTP-84/A068.

12. F. M. Renard, Z. Phys. C1 (1979) 225.

13. J. Lindfors, Shu-Yuan Chu and B. R. Desai, Preprint UCR-TH-84-1 (1984).

14. Such events, i.e. jets associated with photon, have indeed been looked for, preliminarily , in UA1 experiment. R. Kinnunen, private communication.

FIGURE CAPTIONS

Fig. 1. Diagram for $V \to \gamma^*,\ Z^0 \to f\bar{f}$.

Fig. 2. Diagram for $V \to \gamma^*,\ Z^0 \to \ell^+\ell^-$.

Fig. 3. Diagram for $V \to Z^0 \to \nu_\ell \bar{\nu}_\ell$.

Fig. 4. Diagram for $V \to 3g$.

Fig. 5. Diagram for $V \to 2g\gamma$.

Fig. 6. Diagram for $V \to t\bar{t} \to tW^-\bar{b}$.

Fig. 7. Diagram for weak decay $V \to b\bar{b}$.

Fig. 8. Diagram for $V \to H\gamma$, the so-called Wilczek mechanism.

Fig. 9. Diagram for $V \to \gamma^*,\ Z^0 \to H\gamma$.

Fig. 10. Diagram for $V \to \gamma^*,\ Z^0 \to H^3S_1$.

Fig. 11. Diagram for $V \to Z^0 \to H\ell^+\ell^-$.

Fig. 12. Diagram for $V \to \gamma^*,\ Z^0 \to H\gamma$ (composite H).

Fig. 13(a). Diagram for $V \to \gamma^*,\ Z^0 \to H^3S_1$ (composite H).

Fig. 13(b). Diagram for $V \to \gamma^*,\ Z^0 \to H\ell^+\ell^-$ (composite H).

Fig. 14. Decay widths of V into various channels vs. m_t in the minimal model.

Fig. 15. Γ_{W2} and $\Gamma_{W2} + \Gamma_{W3}$ vs. m_t.

Fig. 16. Decay widths of V into channels containing H.

Fig. 17. Contribution of the interference term between the Wilczek and loop diagrams to the decay width of $V \to H\gamma$.

Fig. 18. Branching ratios of V decay into various channel vs. m_t in the minimal model.

Fig. 19. Branching ratios for the decays of V into various channels containing H vs. m_H within the minimal model.

Fig. 20. Branching ratios for various decay channels of V vs. m_t, with enhancement factor $1/\beta = 12$ for the H coupling to fermions and suppression (with the same factor) for the H coupling to $W^{\pm}$, Z^0 bosons.

Fig. 21. Branching ratios of V decay into various channels vs. m_t, in the composite model for Higgs boson.

Fig. 22. Contribution of the interference term between the Wilczek type and the composite diagrams.

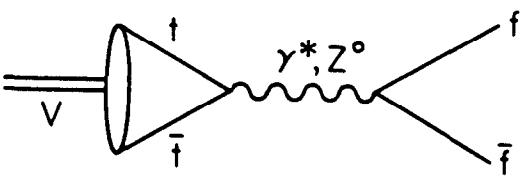

1-85 5016A1

Fig. 1

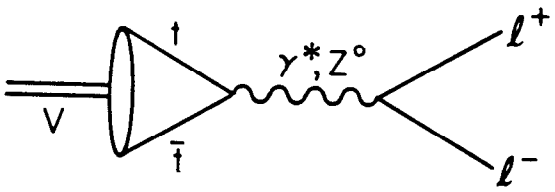

1-85

5016A2

Fig. 2

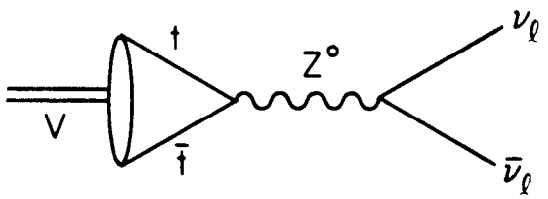

1-85 5016A3

Fig. 3

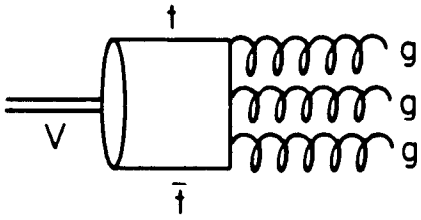

Fig. 4

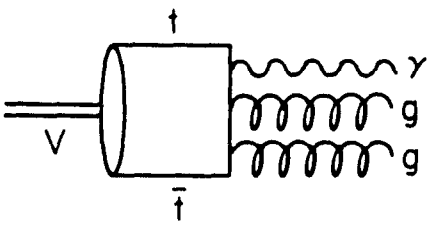

1-85 5016A5

Fig. 5

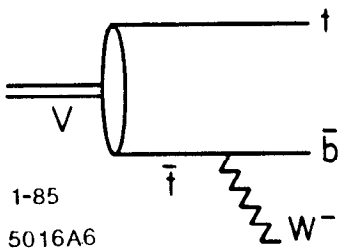

Fig. 6

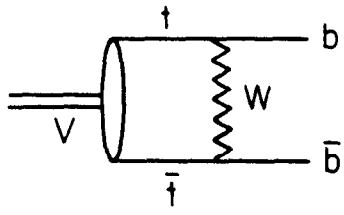

1-85 5016A7

Fig. 7

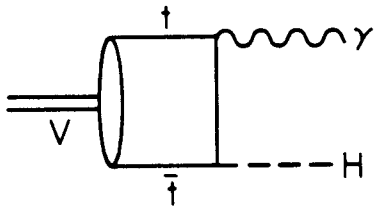

1-85 5016A8

Fig. 8

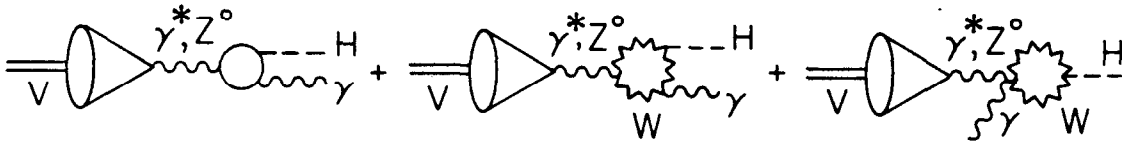

1-85

5016A9

Fig. 9

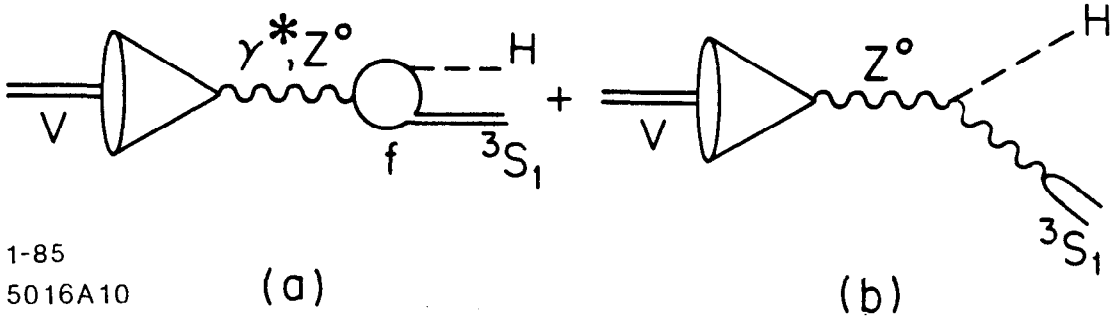

1-85
5016A10

(a) (b)

Fig. 10

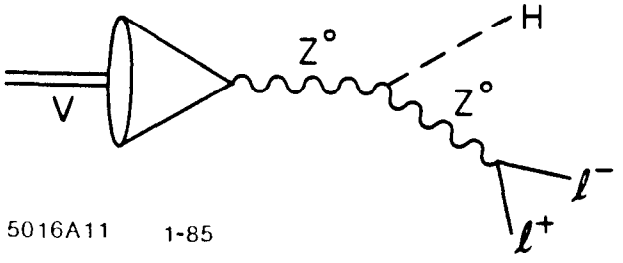

Fig. 11

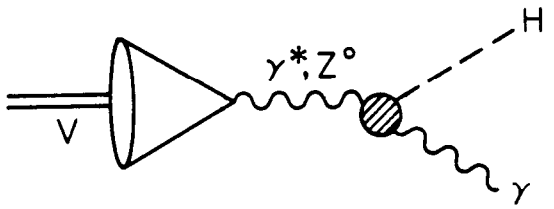

5016A12 1-85

Fig. 12

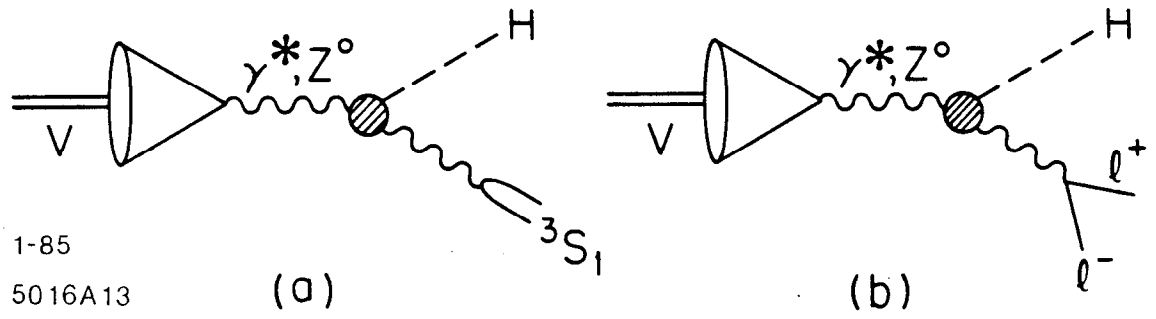

1-85

5016A13

Fig. 13

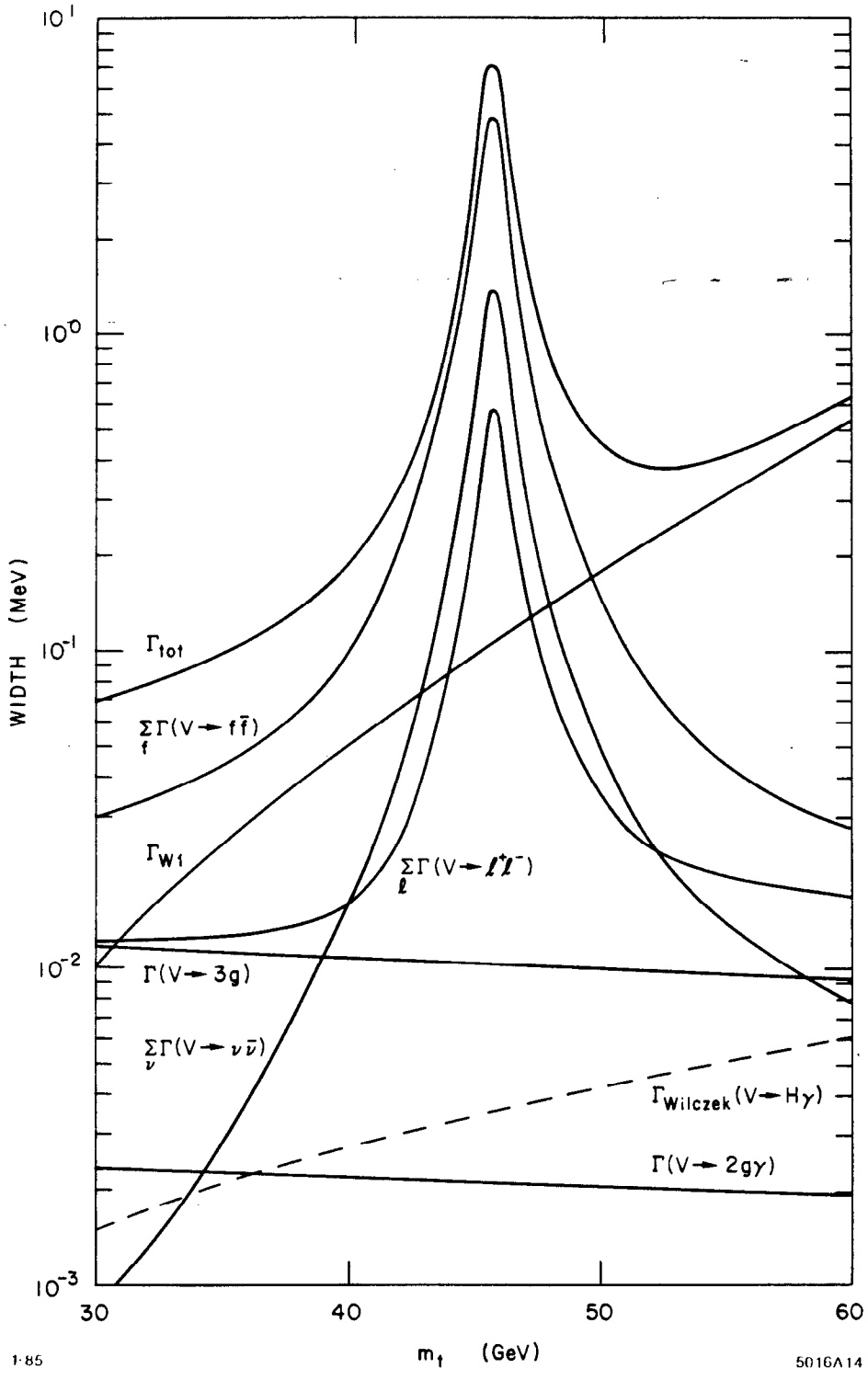
WIDTH (MeV)
10^1
10^0
10^{-1}
10^{-2}
10^{-3}
Γ_{tot}
$\sum_f \Gamma(V \to f\bar{f})$
Γ_{W1}
$\sum_\ell \Gamma(V \to \ell^+\ell^-)$
$\Gamma(V \to 3g)$
$\sum_\nu \Gamma(V \to \nu\bar{\nu})$
$\Gamma_{Wilczek}(V \to H\gamma)$
$\Gamma(V \to 2g\gamma)$
30
40
50
60
m_t (GeV)
1-85
5016A14

Fig. 14

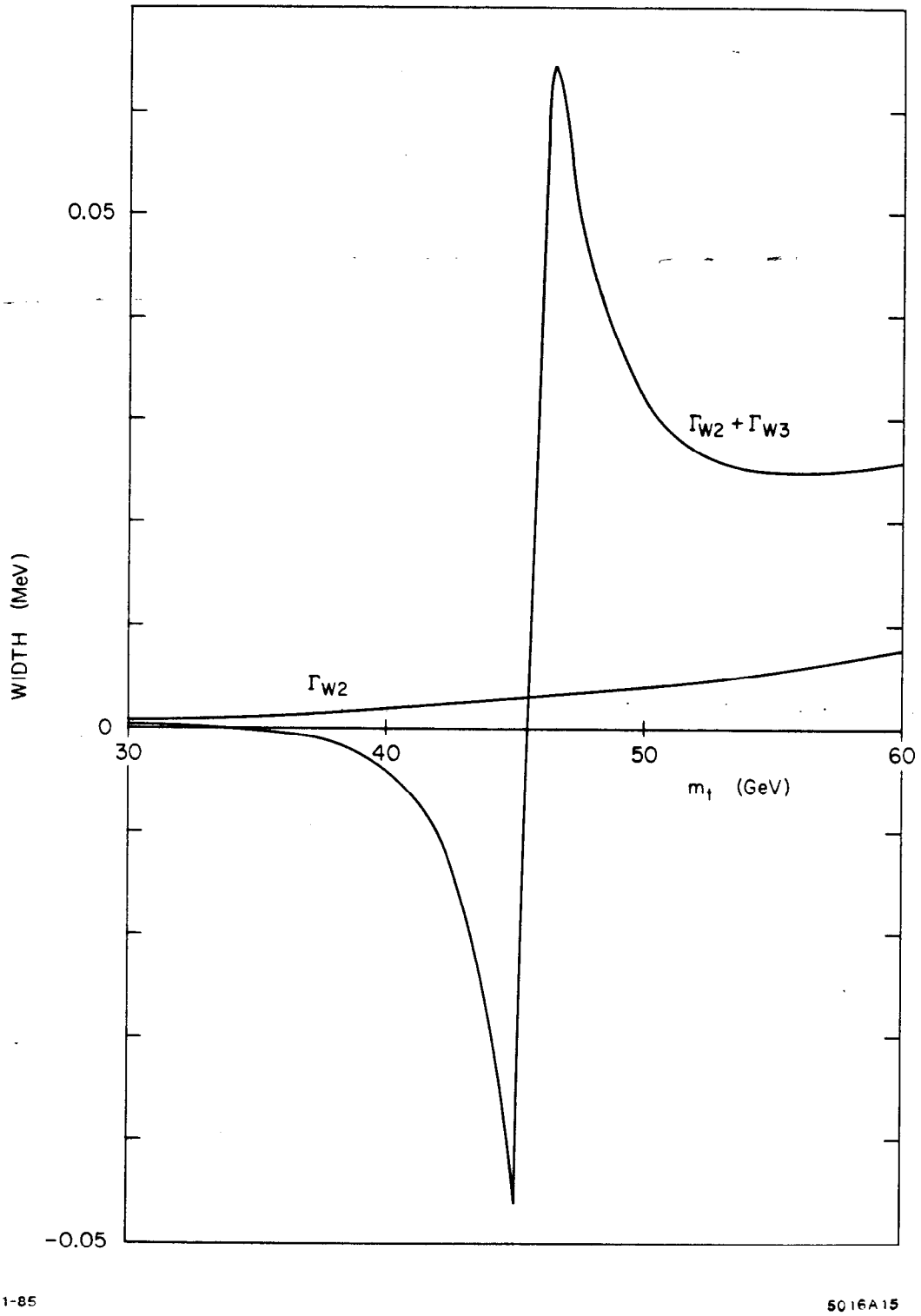
0.05
0
-0.05
WIDTH (MeV)
30
40
50
60
m_t (GeV)
$\Gamma_{W2} + \Gamma_{W3}$
Γ_{W2}
1-85
5016A15

Fig. 15

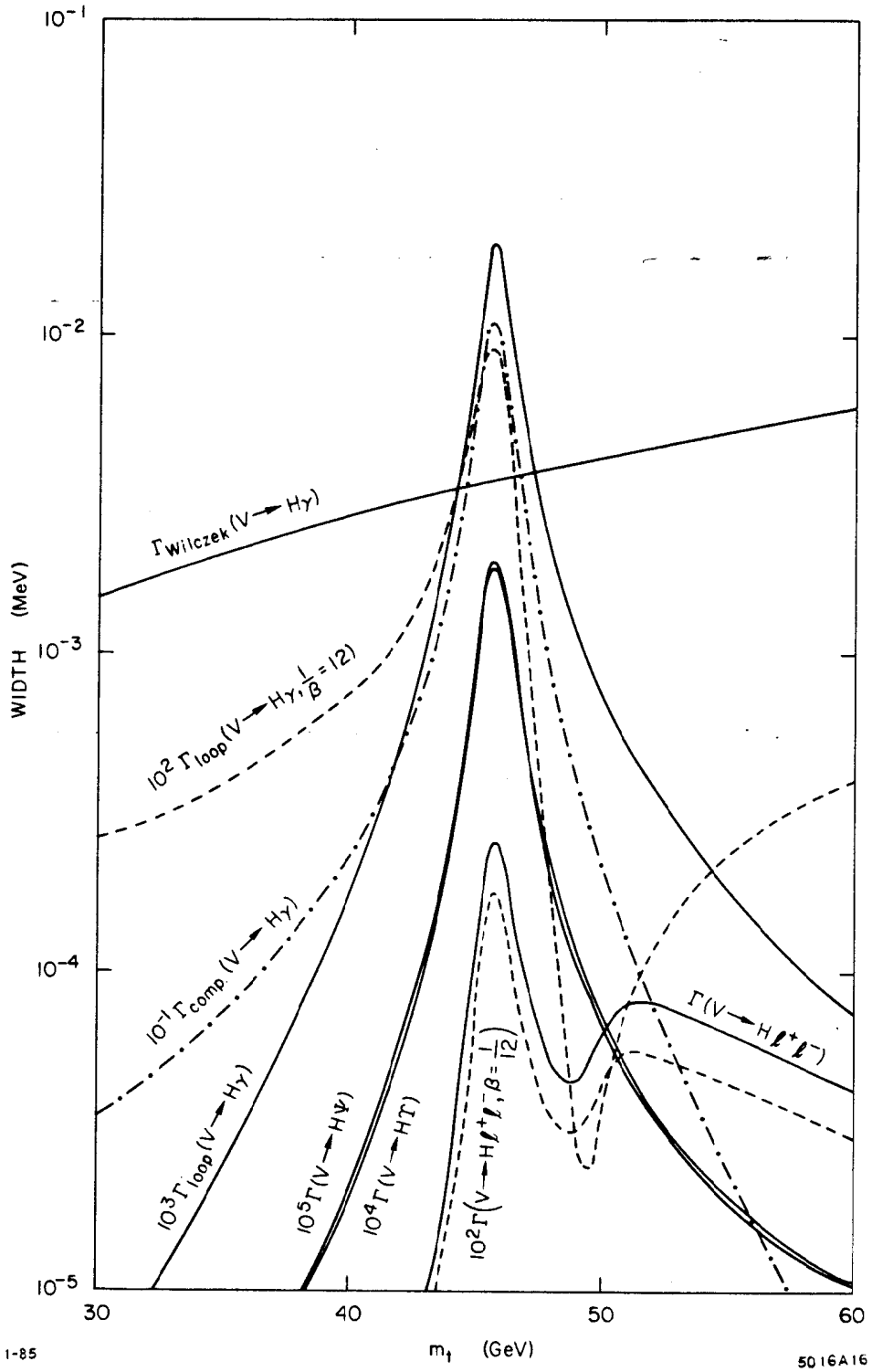
10^{-1}
10^{-2}
10^{-3}
10^{-4}
10^{-5}
WIDTH (MeV)
$\Gamma_{Wilczek}(V \to H\gamma)$
$10^2\,\Gamma_{loop}(V \to H\gamma, \frac{1}{\beta}=12)$
$10^{-1}\,\Gamma_{comp.}(V \to H\gamma)$
$10^3\,\Gamma_{loop}(V \to H\gamma)$
$10^5\Gamma(V \to H\psi)$
$10^4\Gamma(V \to H\Upsilon)$
$10^2\Gamma(V \to H\ell^+\ell^-, \beta=\frac{1}{12})$
$\Gamma(V \to H\ell^+\ell^-)$
30
40
50
60
m_1 (GeV)
1-85
5016A16

Fig. 16

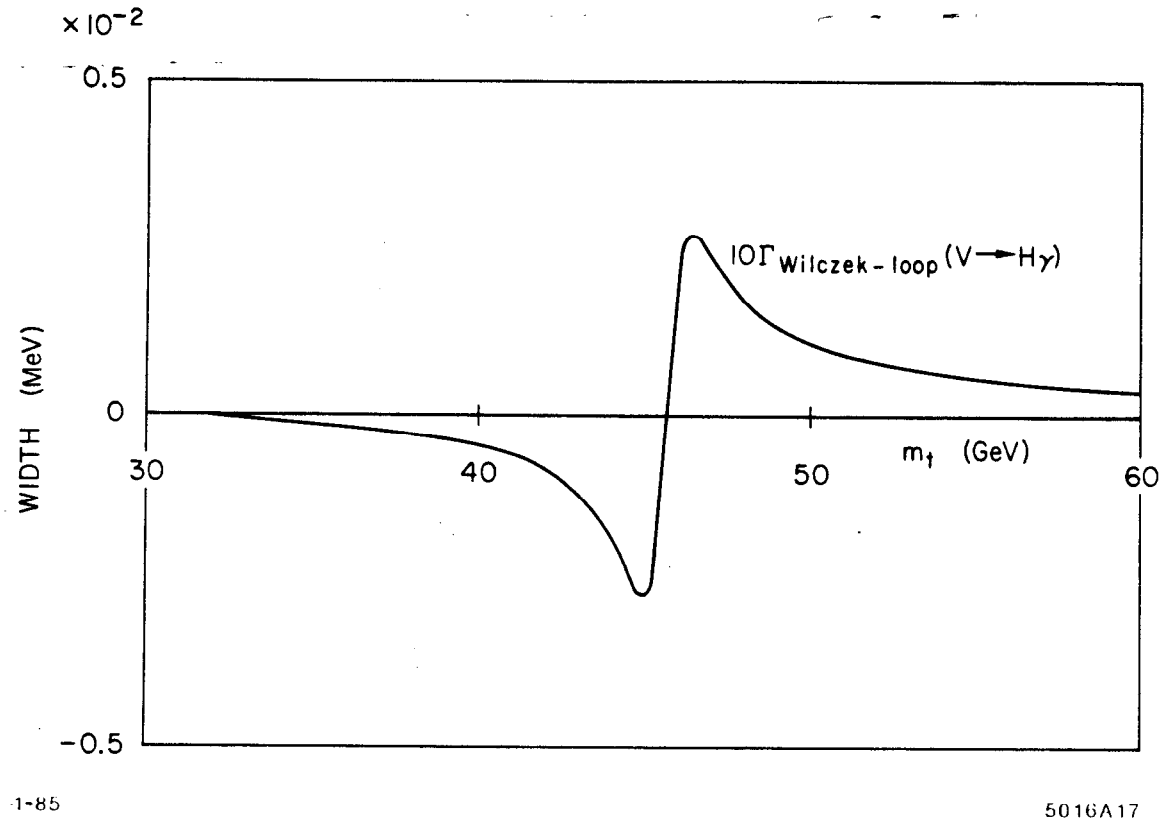
×10⁻²
0.5
0
-0.5
WIDTH (MeV)
10Γ Wilczek - loop (V→Hγ)
30
40
50
60
m_t (GeV)
1-85
5016A17

Fig. 17

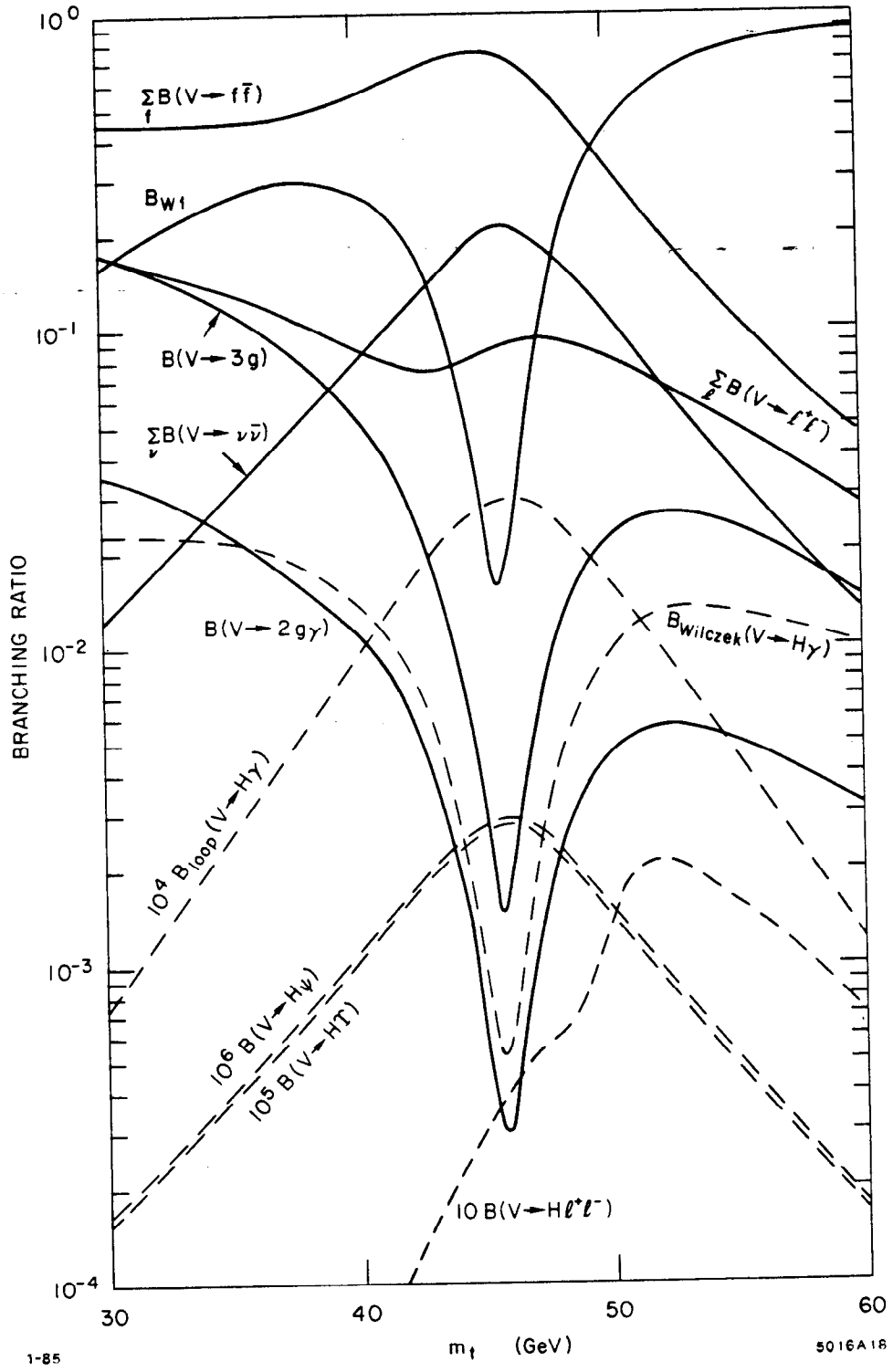
10^0
10^{-1}
10^{-2}
10^{-3}
10^{-4}
BRANCHING RATIO
$\sum_f B(V \to f\bar{f})$
B_{W1}
$B(V \to 3g)$
$\sum_\nu B(V \to \nu\bar{\nu})$
$\sum_\ell B(V \to \ell^+\ell^-)$
$B(V \to 2g\gamma)$
$B_{Wilczek}(V \to H\gamma)$
$10^4\, B_{loop}(V \to H\gamma)$
$10^6\, B(V \to H\psi)$
$10^5\, B(V \to H\Upsilon)$
$10\, B(V \to H\ell^+\ell^-)$
30
40
50
60
m_t (GeV)
1-85
5016A18

Fig. 18

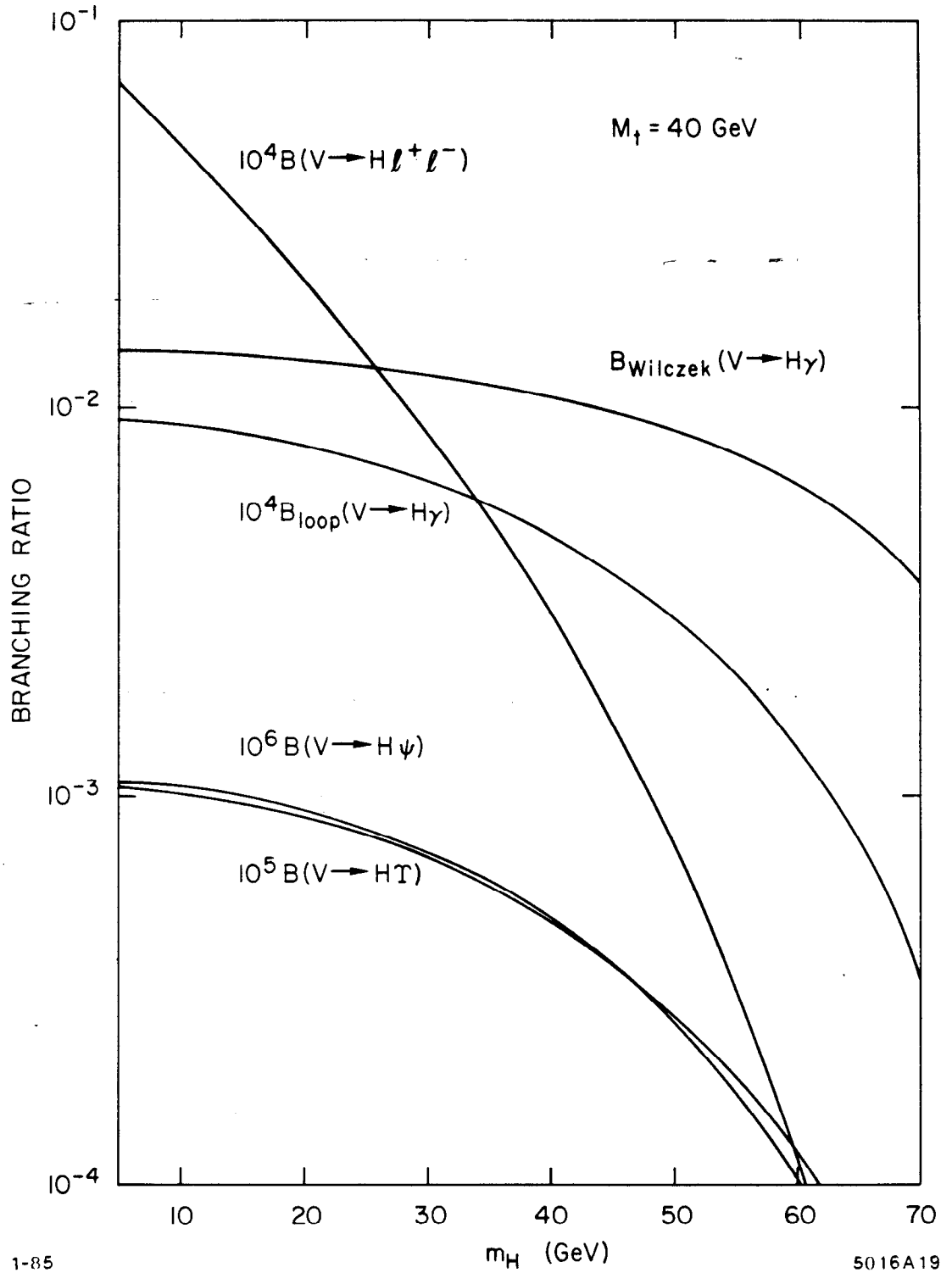
10^{-1}
10^{-2}
10^{-3}
10^{-4}
BRANCHING RATIO
M_t = 40 GeV
$10^4 B(V \rightarrow H \ell^+ \ell^-)$
$B_{Wilczek}(V \rightarrow H\gamma)$
$10^4 B_{loop}(V \rightarrow H\gamma)$
$10^6 B(V \rightarrow H\psi)$
$10^5 B(V \rightarrow H\Upsilon)$
10
20
30
40
50
60
70
m_H (GeV)
1-85
5016A19

Fig. 19

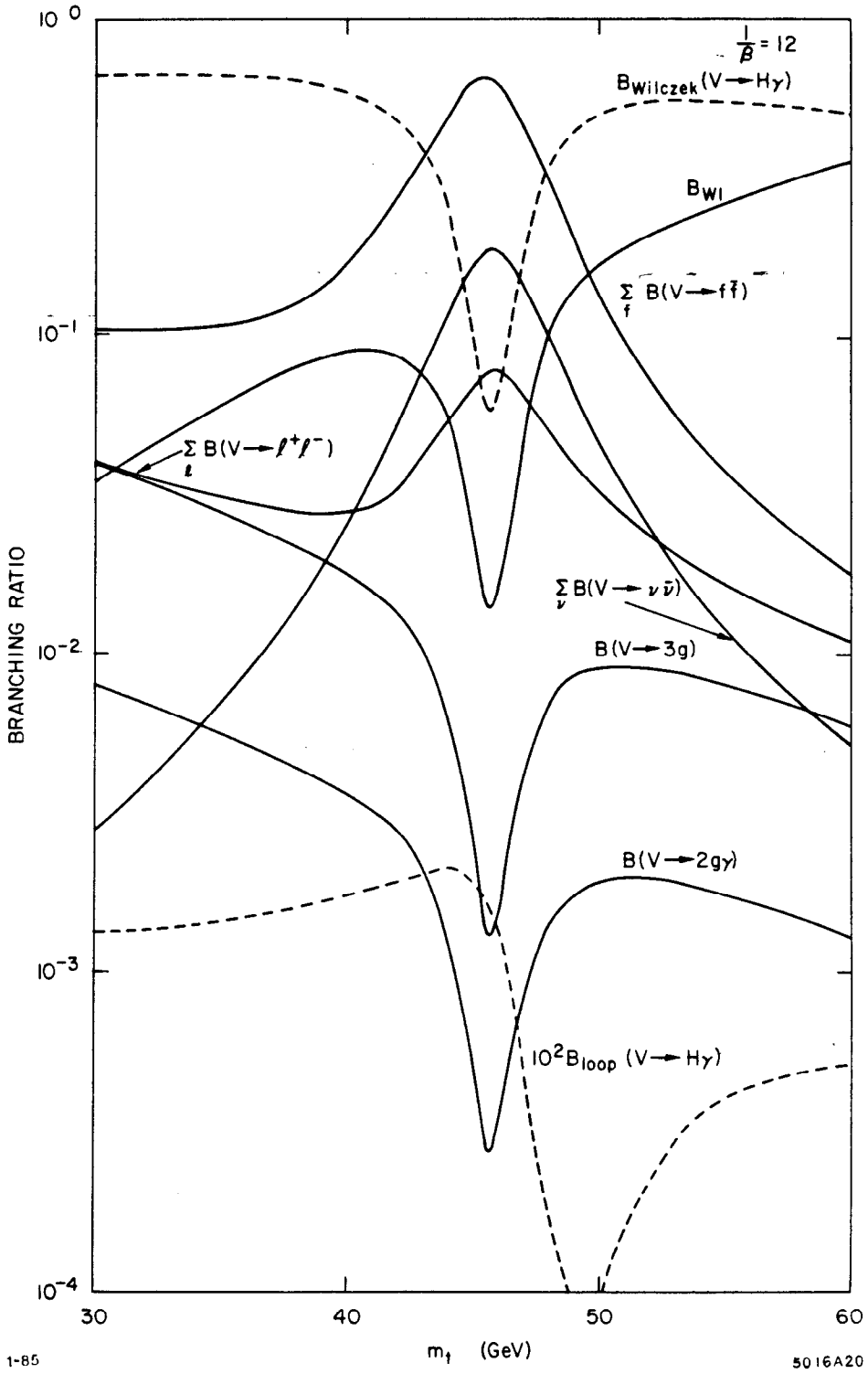
$\frac{1}{\beta} = 12$
$B_{Wilczek}(V \to H\gamma)$
B_{WI}
$\sum_f B(V \to f\bar{f})$
$\sum_l B(V \to l^+l^-)$
$\sum_\nu B(V \to \nu\bar{\nu})$
$B(V \to 3g)$
$B(V \to 2g\gamma)$
$10^2 B_{loop}(V \to H\gamma)$
BRANCHING RATIO
10^0
10^{-1}
10^{-2}
10^{-3}
10^{-4}
30
40
50
60
m_t (GeV)
1-85
5016A20

Fig. 20

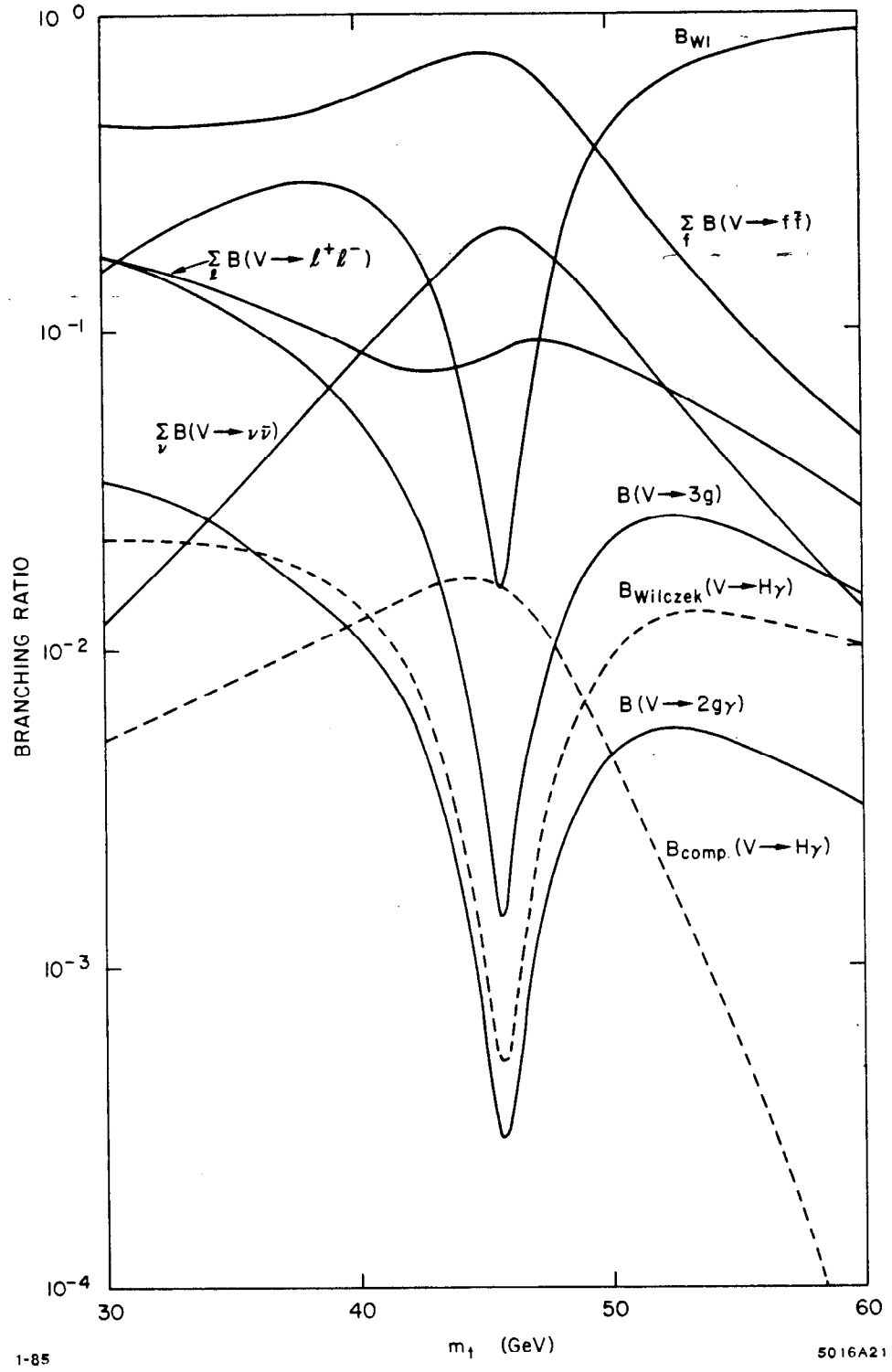
10^0
10^{-1}
10^{-2}
10^{-3}
10^{-4}
BRANCHING RATIO
B_{WI}
$\sum_f B(V \to f\bar{f})$
$\sum_\ell B(V \to \ell^+\ell^-)$
$\sum_\nu B(V \to \nu\bar{\nu})$
$B(V \to 3g)$
$B_{Wilczek}(V \to H\gamma)$
$B(V \to 2g\gamma)$
$B_{comp.}(V \to H\gamma)$
30
40
50
60
m_t (GeV)
1-85
5016A21

Fig. 21

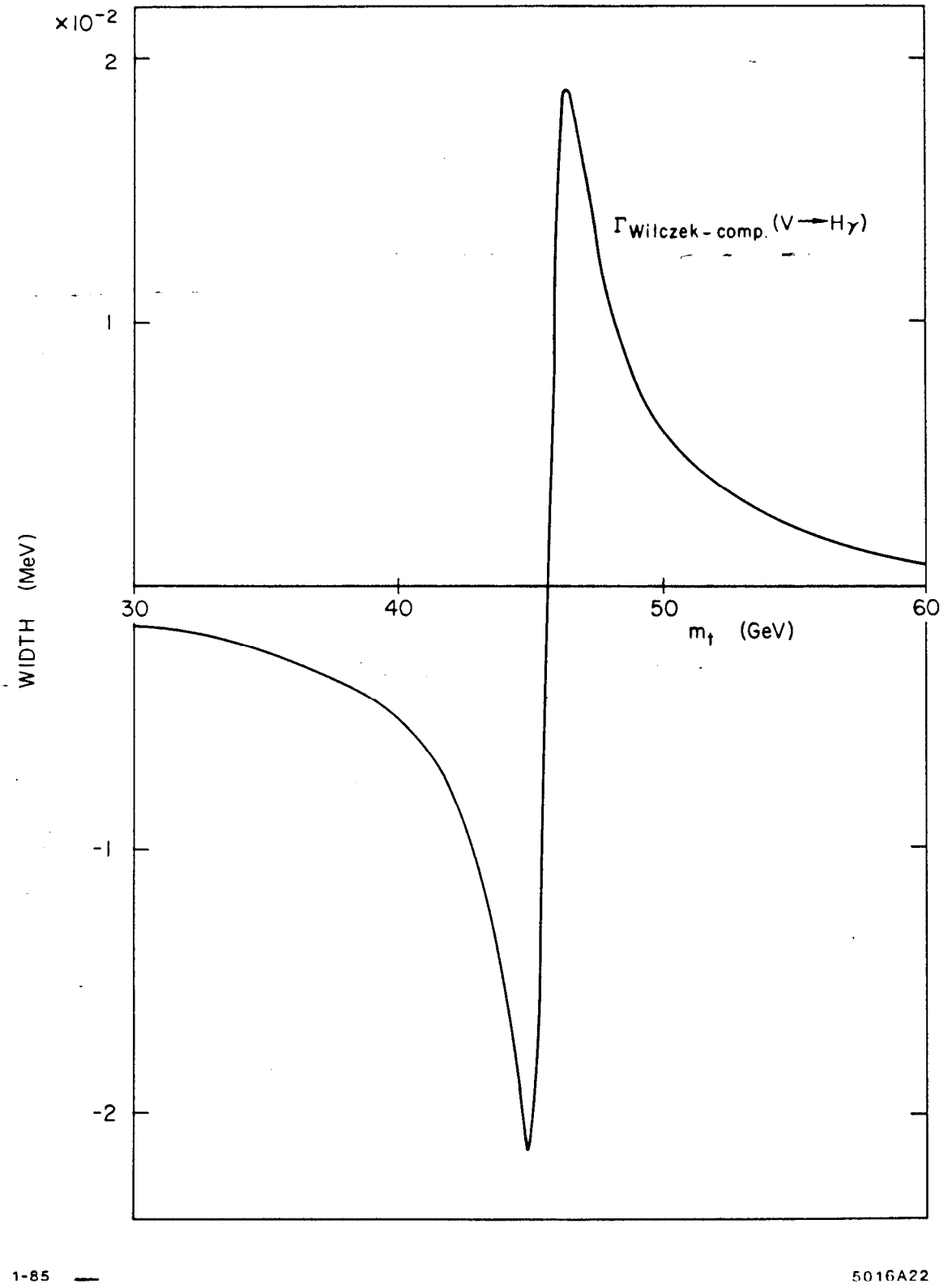
×10⁻²
2
1
-1
-2
WIDTH (MeV)
30
40
50
60
m_t (GeV)
$\Gamma_{Wilczek-comp.}(V \rightarrow H\gamma)$
1-85
5016A22

Fig. 22